Theor Chem Acc (2011) 128:639–646
DOI 10.1007/s00214-010-0823-6

REGULAR ARTICLE

The importance of conformational search: a test case on the catalytic cycle of the Suzuki–Miyaura cross-coupling

Maria Besora · Ataualpa A. C. Braga · Gregori Ujaque · Feliu Maseras · Agustí Lledós

Received: 2 July 2010 / Accepted: 13 September 2010 / Published online: 29 September 2010

Abstract Conformational diversity is an often neglected aspect in computational studies of transition metal complexes, even when relatively large systems are involved. The importance of conformational searches is illustrated through the analysis of the errors that could be caused by a wrong choice of conformers in the computational study of the Suzuki–Miyaura cross-coupling between CH_2=CHBr and CH_2=CHB(OH)$_2$ catalyzed by [(PPh$_3$)$_2$Pd] or [(P(*i*-Pr)$_3$)$_2$Pd]. The error bars associated with conformational diversity of the [(PPh$_3$)$_2$Pd] catalyst range between 0.3 and 6.7 kcal/mol, the values growing up to 11.4 kcal/mol when the more flexible [(P(*i*-Pr)$_3$)$_2$Pd] catalyst is considered.

Keywords Conformational searches · Cross-coupling · DFT · DFT/MM

Published as part of the special issue celebrating theoretical and computational chemistry in Spain.

Electronic supplementary material The online version of this article (doi:10.1007/s00214-010-0823-6) contains supplementary material, which is available to authorized users.

M. Besora · A. A. C. Braga · F. Maseras (✉)
Institute of Chemical Research of Catalonia (ICIQ),
Av. Països Catalans 16, 43007 Tarragona, Catalonia, Spain
e-mail: fmaseras@iciq.es

G. Ujaque · F. Maseras · A. Lledós (✉)
Departament de Química, Edifici Cn,
Universitat Autònoma de Barcelona,
08193 Bellaterra, Catalonia, Spain
e-mail: agusti@klingon.uab.es

1 Introduction

The accuracy of relative energies continues to be a challenge for computational chemistry. The application of density functional theory (DFT) to molecular systems of practical interest usually raises questions on the appropriateness of the functional and the size of the basis set, with other topics, such as solvation models or free energy corrections often being considered [1–3]. Conformational diversity is however seldom taken into account. Chemical species may exist in several conformers, interconnected by low energy barriers, and we are usually interested only in the most stable one, the global minimum. In the early days of computational chemistry, the systems that could be studied were quite small, and chemical knowledge and the use of simple drawings were sufficient to sort out conformational issues. Luckily nowadays, we are able to perform reliable calculations on large systems. The number of conformers becomes difficult or impossible to manage by use of sheer patience and chemical intuition, and automated conformational searches need to be performed.

Conformational searches do require an extra-effort and the use of slightly different computational tools, but are by no means an impossible task. Molecular mechanics (MM) force fields are extremely useful in this context. Things can be more complicated when transition metal atoms are involved, but solutions are nevertheless available [4–6], either by careful parameterization of the metal and ligand before performing the search [6–9] or by carefully freezing the coordination sphere of the metal centre and searching conformations on the rest [10–14].

In the present contribution, we try to estimate the error bars associated with conformational diversity in the computational study of a well-known catalytic cycle. Some of us already stressed a few years ago the importance of

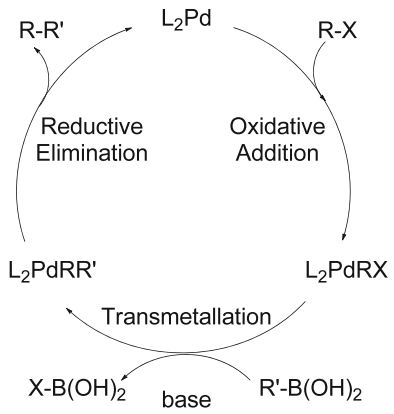

Fig. 1 Schematic representation of the Suzuki–Miyaura catalytic cycle

conformational searches when carrying computational studies on large systems, for the case of the structure of the $[OsH_2Cl_2(P(i\text{–}Pr)_3)_2]$ transition metal complex [15]. Others have also pointed to the importance of performing conformational searches [6, 16].

The reaction chosen for this work is the catalytic cycle of the Suzuki–Miyaura cross-coupling [17–23]. This reaction couples an organic halide and an organoboron compound by means of a palladium catalyst in the presence of a base. The main steps of the reaction are oxidative addition [24–28] of the organic halide, a transmetalation [29–31] step assisted by the base and reductive elimination [32–35] (see, Fig. 1).

The catalyst is usually a phosphine-based palladium complex. Depending on the nature of the phosphine used, the reaction is expected to be catalyzed by a bis- or monophosphine complex [36–40]. The current study considers two possible bis-phosphine catalysts $[(PPh_3)_2Pd]$ and $[(P(i\text{–}Pr)_3)_2Pd]$. The chosen organic halide and organoborane are CH_2=CHBr and CH_2=CHB$(OH)_2$, mainly because they are simple, already studied and computationally cheap. The full catalytic cycle with PH_3 as model for the phosphines was already studied by some of us [40–42].

2 Computational details

Conformational searches were performed using the MacroModel 8.5 [43] program as available from Schrödinger LLC. The conformational search method used was Monte Carlo Multiple Minimum (MCMM) [44, 45]. The parameters were 1,000 evaluation steps and an energy window of 12.0 kcal/mol (50 kJ/mol). The MM3 force field [46] was applied. During the conformational search, a number of atoms were frozen to the relative positions obtained on a previous QM optimization on a model system. This included the Pd, P and Br atoms, as well as other atoms such as the carbons of the CH=CH_3 groups bonded to Pd. A large number of structures were obtained, some of them repeatedly. They were screened and analyzed by visual inspection and through the use of the Xcluster [47] program, also from Schrödinger LLC. For each species, a number between 20 and 40 structures were selected for recalculation at a QM/MM level.

QM/MM calculations were performed using ONIOM [48, 49] as available in Gaussian 03 [50]. The species were divided in two regions: QM and MM. The high-level QM region included all the atoms except phenyl or isopropyl substituents and was treated with DFT using the B3LYP functional [51–53]. The basis sets used were the standard split–valence polarized 6–31G(d, p) basis sets [54–56] for most atoms. For Pd, Br and P, the SDD valence basis set with the associated Stuttgart/Dresden effective core potentials was used [57–60]. The MM region was treated with UFF [61]. It only included the phenyl and isopropyl substituents of the phosphine ligands.

For some of the transition states and intermediates, six QM/MM conformers (the three most and least stable) were re-optimized at full QM level using the same level of theory as the one described for the QM region of the QM/MM calculations.

Geometries of the most stable isomer located for each species at QM/MM and QM level are collected in the Supporting Information.

3 Results

The catalytic cycle of the Suzuki–Miyaura cross-coupling, as stated above, is generally accepted to have mainly three different steps: the oxidative addition, the transmetallation and the reductive elimination, see Fig. 1. The present study does not want to enter into the discussion of the mechanism itself, but just on the effects that the conformational diversity of the species along the catalytic cycle may have on the conclusions of computational studies. No discussion of phosphine dissociation, effect of the base, isomerization and other mechanistic possibilities will be performed, and mainly the conclusions reached for the model system $[(PH_3)_2Pd]$, CH_2=CHBr, CH_2=CHB$(OH)_2$ with the base OH^- will be extrapolated to the two catalysts considered, $[(PPh_3)_2Pd]$ and $[(P(i\text{-}Pr)_3)_2Pd]$ [40].

The results have been generated with an energy window of 12 kcal/mol, see computational details. This energy window is a compromise that should allow us to generate several conformers with reasonable rearrangements and at the same time avoid improbable geometries. The idea is to focus on geometries one could draw following chemical intuition and avoid the ones against it. From the 20–40 structures coming from the conformational search, after

QM/MM optimization, 12–18 conformers with different energy remained for the [$(PPh_3)_2Pd$] catalyst and around 20–30 for the [$(P(i\text{-}Pr)_3)_2Pd$]. This QM/MM intermediate step was not strictly necessary, but it allowed the elimination of some unrealistic minima emerging from the constrained MM search and reduced the number of steps in the subsequent QM calculations. Further optimization at QM level of the three most and three least stable structures leads to 4–5 different structures for the [$(PPh_3)_2Pd$] catalyst and 6 for the [$(P(i\text{-}Pr)_3)_2Pd$].

3.1 [$(PPh_3)_2Pd$] catalyst

An energy profile of the catalytic cycle is presented in Fig. 2. The oxidative addition of CH_2=CHBr to [$(PPh_3)_2Pd$] (**1**) starts by formation of an adduct [$(PPh_3)_2Pd(\pi$–CH_2=CHBr)] (**2**) where the interaction between the palladium metal centre and the reactant is achieved through the C=C bond. The transition state **TSOA** breaks the C–Br bond forming the square-planar structure *cis*– [$(PPh_3)_2Pd(Br)(CH{=}CH_2)$] (**3-cis**). The conformers of **1** have been located over a small range of energies, 0.3 kcal/mol, much narrower than the original conformational search window. The linear geometry of the P–Pd–P angle is able to accommodate easily the different conformations of the PPh_3 ligands. Adduct **2** has a trigonal-planar geometry. The coordination of CH_2=CHBr makes the coordination sphere more crowded, and consequently, the different conformers cover a slightly wider range of 1.1 kcal/mol. In the transition state **TSOA**, where the C–Br bond is broken and the Pd–C and Pd–Br bonds are formed, the conformers are found over a range of 1.4 kcal/mol. The lowest energy conformer of **TSOA** is presented in Fig. 3. The conformers of the **3-cis** intermediate can be found over a larger range of 3.2 kcal/mol. The *cis* arrangement of the phosphines results in a more constrained system.

The oxidative addition is the rate-limiting step of the reaction, with a barrier of 19.1 kcal/mol at QM/MM level. By random choice of conformers, the barrier could oscillate between 18.0 and 20.5 kcal/mol. 18.0 kcal/mol would be obtained when taking the highest energy conformer of **2** and the lowest energy conformer of **TSOA**, and 20.5 kcal/mol when doing the opposite. Thus, the barriers found by random combination of structures could vary as much as 2.5 kcal/mol.

The **3-cis** complex can isomerize to **3-trans**. The **3-trans** complex presents the different conformers in a smaller range of 1.6 kcal/mol. This is because the phosphines are easier to accommodate in the *trans* complex. There are different alternative mechanisms to perform such isomerization as has been discussed previously [40, 62], but the barriers are low. For the PH_3 model system, the barrier was evaluated in 5.5 kcal/mol. We did not analyze the conformational diversity in this step, and for this reason, it is represented in Fig. 2 with a dashed line.

The transmetalation step can take place through two parallel pathways, starting from either the **3-cis** or the **3-trans** isomers formed after the oxidative addition. It has

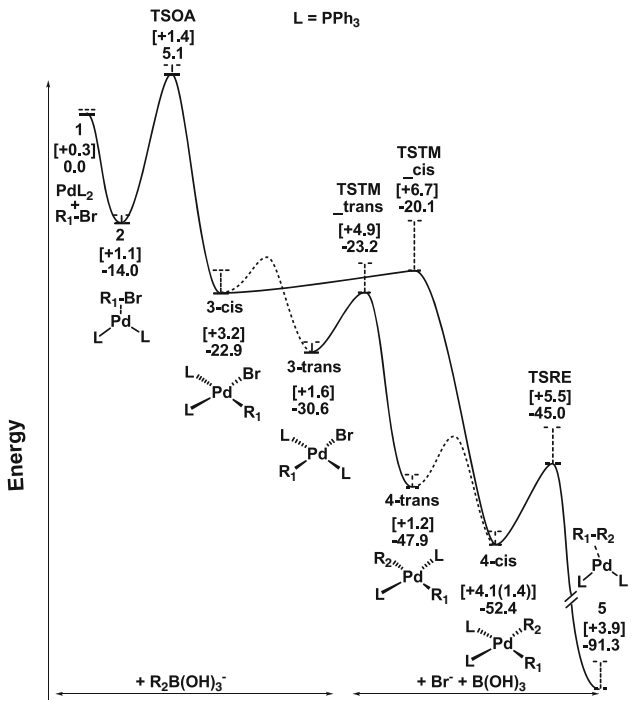

Fig. 2 Schematic potential energy profile of the catalytic cycle for the [$(PPh_3)_2Pd$] (L_2Pd) catalyzed cross-coupling between CH_2=CHBr (R_1–Br) and $CH_2{=}CHB(OH)_3^-$ (R_2–$B(OH_3)^-$), in kcal/mol. In brackets, the energy difference between the most and the least stable conformers for each species is given. Dashed curves show approximate barriers for the isomerization steps that have not been considered in this work

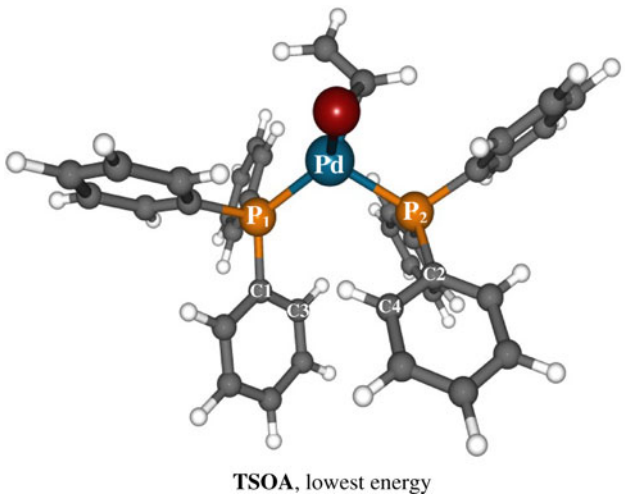

TSOA, lowest energy

Fig. 3 Geometry of the lowest energy conformer of **TSOA** at QM level

been shown that in both cases, the transmetalation involves different intermediates and transition states, but that where the carbon–boron bond is cleaved has the highest energy [13, 14]. The present study focuses only on this specific transition state, which has been labeled as **TSTM**. In **TSTM**, two phosphines and a vinyl are coordinated to the metal centre. The fourth site of the square-planar structure is occupied by the CH_2=CHB$(OH)_3^-$, and it is in this site where C–B bond cleavage and Pd–C bond formation take place. The isomers corresponding to each of the pathways are labeled as **TSTM_cis** and **TSTM_trans**. The conformers of the **TSTM_cis** species occupy a range of 6.7 kcal/mol, while those of **TSTM_trans** are in a range of 4.9 kcal/mol. The larger range for **TSTM_cis** is due to the higher steric constrains, because of the *cis* organization of the phosphines, coupled with the presence of the large CH_2=CHB$(OH)_3^-$ group. **TSTM_trans** is 2.8 kcal/mol below **TSTM_cis** when the most stable conformers are considered. With a random choice of conformers, this energy difference may oscillate between −2.1 and +9.5 kcal/mol. This is a particular case when the wrong choice of conformers could lead to an incorrect prediction of the reaction mechanism.

The transmetalation step leads to intermediate [$(PPh_3)_2$Pd$(CH{=}CH_2)_2$] (**4**). This species can be *cis* or *trans*, being the *cis* isomer the most stable. The conformers of **4-trans** can be found over a range of 1.2 kcal/mol, while the ones of **4-cis** cover a range of 4.1 kcal/mol. The *cis*/*trans* isomerization has not been studied in the present work. It was previously reported to have a barrier of 9.6 kcal/mol for the PH_3 model system [13].

Only the **4-cis** isomer can lead directly to the product after the reductive elimination step. The transition state for this process **TSRE** involves the elimination of the two Pd–C bonds and the formation of the C–C bond. The conformers of this transition state have energies spread over a range of 5.5 kcal/mol. This high value is likely associated with the flexibility in the orientation of the vinyl groups. After the reductive elimination, an adduct [$(PPh_3)_2$Pd$(\pi$–$CH_2{=}CHCH{=}CH_2)$] (**5**) is formed. The conformers of this species are found in a range of 3.9 kcal/mol, quite large compared with **2**, mainly due to the conformational changes of the CH_2=CHCH=CH_2 chain.

If we consider the process as a whole, the effects of overlooking conformational diversity can be significant. The barrier of the rate-limiting step could be increased or decreased by about 1.5 kcal/mol, the preference between the *cis* or *trans* pathways for transmetalation could be inverted, and the barrier for the reductive elimination altered by more than 4 kcal/mol.

Some of the conformers of the more relevant species were recomputed at full QM level. The relative energies with respect to **1** and CH_2=CHBr and CH_2=CHB$(OH)_3^-$ of **2**, **TSOA**, **TSTM_cis** and **TSTM_trans** were −12.5, +4.0, −15.6, −19.9 kcal/mol, respectively. The energy ranges between the least, and the most stable conformers are 0.1, 0.4, 2.5, 9.3 and 4.0 kcal/mol for **1**, **2**, **TSOA**, **TSTM_cis** and **TSTM_trans**. The differences between these energies and the ones found at QM/MM level can be attributed to the introduction of electronic effects in the QM calculation.

Five conformers of **TSOA** are further analyzed in Table 1. Their relative energies and some relevant geometrical parameters are presented as an example of the variety of conformers generated. The geometry of the lowest energy conformer (**TSOA a**) is presented in Fig. 3. It can be observed that the geometrical parameters corresponding to the formation/cleavage of bonds in the transition state, Pd–C and Pd–Br distances, do not change much in the different conformers (values change just 0.030 and 0.009 Å, respectively). The P–Pd–P angle has also small variations (5.5°). The C_1–P_1–P_2–C_2 dihedral angle (atom labeling from Fig. 3) is used as a relative measure of how eclipsed or staggered are the phosphine substituents. Conformers **TSOA a**, **TSOA c** and **TSOA e** are less eclipsed than **TSOA b** and **TSOA d**. This parameter alone is not sufficient to distinguish among the different conformers as **TSOA a** and **TSOA e** have similar angles and quite different energies. Two Pd–P–C–C dihedral angles, giving an idea of the phenyl orientation, are also included in Table 1. The values for the Pd–P_1–C_1–C_3 and Pd–P_2–C_2–C_4 show a large diversity between the different conformers. The factors that make **TSOA a** the most stable conformer are complex and correspond to a compensation of different factors. Chemical intuition and observation of simple chemical rules will be often insufficient to identify the most stable conformer.

Table 1 Relative energies (kcal/mol) and selected parameters (distances in Å, angles in °) of the QM optimized conformers of **TSOA**

	ΔE_{QM} (kcal/mol)	Pd–C (Å)	Pd–Br (Å)	P–Pd–P (°)	C_1–P_1–P_2–C_2 (°)	Pd–P_i–C_i–C_{i+2} $i = 1; 2$ (°)
a	4.0	1.985	2.836	111.0	37.6	−63.5; 23.8
b	4.1	1.996	2.827	116.5	11.6	−38.7; −23.4
c	4.1	1.997	2.829	113.0	44.5	54.8; −28.4
d	4.5	1.994	2.829	115.5	15.5	35.3; 38.5
e	6.5	2.005	2.834	115.0	33.8	−22.9; −77.1

Labels according to Fig. 3

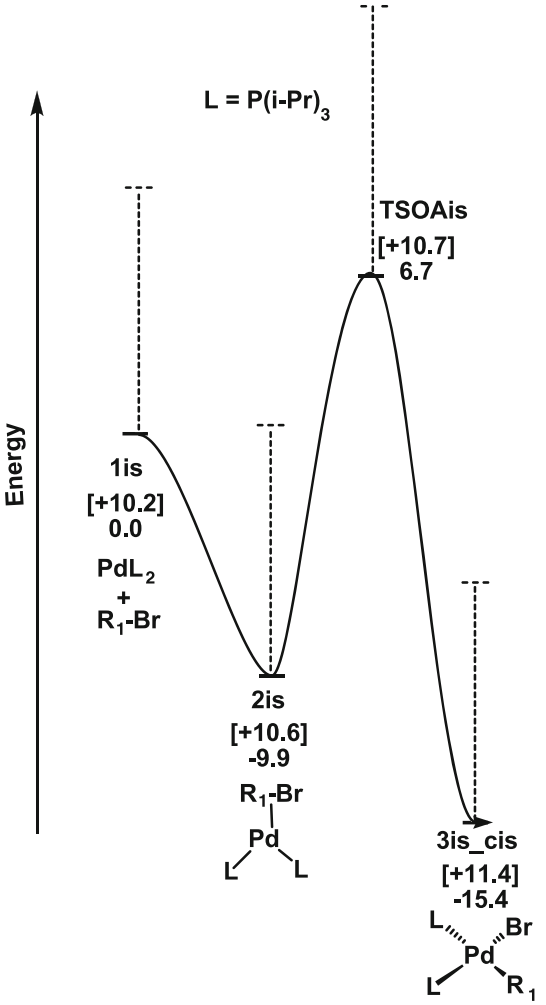

Fig. 4 Schematic potential energy profile of oxidative addition of CH_2=CHBr (R_1–Br) to [(P(*i*-Pr)$_3$)$_2$Pd] (L_2Pd), in kcal/mol. In brackets, the energy difference between the least and the most stable conformer for each species is given

3.2 [(P(*i*-Pr)$_3$)$_2$Pd] catalyst

When the phenyl groups are replaced by the bulkier isopropyl groups, the conformers can be found over a larger range of energies. Not all the catalytic cycle has been recomputed for this catalyst [(P(*i*-Pr)$_3$)$_2$Pd], and just the oxidative addition has been considered. A schematic energy profile containing only the results for this step is presented in Fig. 4.

The [(P(*i*-Pr)$_3$)$_2$Pd] complex (**1is**) reacts with CH_2=CHBr to form the adduct [(P(*i*-Pr)$_3$)$_2$Pd(π–CH_2=CHBr)] (**2is**). The oxidative addition takes place through the transition state **TSOAis** forming the intermediate cis-[(P(*i*-Pr)$_3$)$_2$Pd(Br)(CH=CH_2)] **3is-cis** that can isomerize to the most stable **3is-trans**.

The conformers of the catalyst **1is** can be found over a range of 10.2 kcal/mol, showing a large variety of

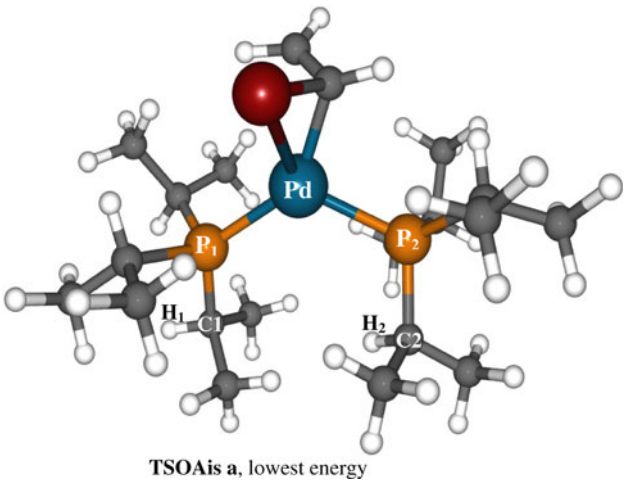

TSOAis a, lowest energy

Fig. 5 Geometry of the lowest energy conformer of **TSOAis** at QM level

structures. Similarly, the conformers of the adduct **2is** and the transition state **TSOAis** (see Fig. 5) can be found over a range of 10.6 and 10.7 kcal/mol, respectively. The product of the oxidative addition **3is-cis** presents conformers over a range of 11.4 kcal/mol. It is clear that the ranges of energies of the different conformers when tris(isopropyl) phosphine is involved are much larger than for triphenylphosphine, where the maximum range for the oxidative addition was 3.2 kcal/mol. This is due to the specific geometry of the isopropyl substituent, which can lead to well-packed conformers or crowded ones. Remarkably, in the case of P(*i*-Pr)$_3$, the computed range is very similar to the energy window in the MacroModel search. Thus, for P(*i*-Pr)$_3$, the conformational diversity is sufficient to occupy the full window, and the energy range may have been larger had a wider window been considered.

The large error bars indicated in Fig. 4 lead to wide oscillations of the computed barrier for randomly chosen conformations. The computed QM/MM barrier between the most stable conformers of 15.6 kcal/mol between **2is** and **TSOAis** could oscillate between 6.0 and 27.3 kcal/mol with a bad choice of conformers.

Full QM calculations were performed over a few of the conformers at the extremes of the energy range for **1is**, **2is** and **TSOAis**. The energy ranges for the re-optimized conformers are 9.3, 8.1 and 8.7 kcal/mol, respectively. The geometry of the lowest energy conformer of **TSOAis** at QM level is presented in Fig. 5. These ranges of energies are slightly narrower than those found for the QM/MM calculations, but the distribution is still wide and quite close to the window initially used in the conformational search.

The relative energies and some geometrical parameters for the six QM optimized conformers of **TSOAis** are presented in Table 2. The Pd–C and Pd–Br distances, as well

Table 2 Relative energies (kcal/mol) and selected parameters (distances in Å, angles in °) of the QM optimized conformers of **TSOAis**

	ΔE_{QM} (kcal/mol)	Pd–C (Å)	Pd–Br (Å)	P–Pd–P (°)	C_1–P_1–P_2–C_2 (°)	Pd–P_i–C_i–H_i $i = 1; 2$ (°)
a	9.1	2.016	2.850	122.6	28.2	−178.1; 54.3
b	11.6	2.009	2.822	117.5	31.2	−90.4; 174.0
c	11.7	2.009	2.825	118.4	28.8	78.9; −68.6
d	15.5	2.015	2.868	120.4	6.3	44.2; 40.6
e	16.0	2.011	2.871	125.7	9.7	82.5; 44.4
f	17.8	2.003	2.843	118.6	19.6	48.5; 41.1

Labels according to Fig. 5

as the P–Pd–P angle, do not present large variations among the conformers. P–Pd–P angles are larger for **TSAOis** than they were for **TSAO** (117.5–125.7° vs. 111.0–116.5°). This can be explained by the different steric bulk of the ligands, as described by Tolman cone angles ($P(i\text{-}Pr)_3$160°, PPh_3 145°) [63]. The C–P–P–C dihedral angle can be used as a measure of how eclipsed or staggered are the phosphines. We can observe that the three lowest energy conformers **TSOAis a–c** present dihedrals of around 30°, while the three least stable **TSOAis d–f** present smaller dihedral angles. This indicates a more eclipsed arrangement of the least stable conformers, consistent with a higher steric hindrance. In Table 2, we also report two of the Pd–P–C–H dihedral angles. There are of course four other Pd–P–C–H torsions, but a general picture can already be extracted from the two presented. Different conformers show a variety of arrangements of the isopropyl substituents. In the most stable structures, **TSOAis a** and **b,** one of the dihedral angles is close to 180°. There seems to be a general trend favouring this arrangement, but other effects play obviously important roles. **TSOAis a** is 2.5 kcal/mol more stable than **TSOAis b**, and **TSOAis c**, with a very similar energy to **TSOAis b**, does not present such type of arrangement. Again, chemical intuition and simple rules cannot determine a priori which the global minimum is.

We find a large dispersion of conformational energies for the system with the $[(P(i\text{-}Pr)_3)_2Pd]$ catalyst. This result was to be expected. Compared to $[(PPh_3)_2Pd]$, the system has a larger conformational complexity. For each phenyl substituent, there is practically only one variable to consider, namely the torsion around the P–C bond. On the other had, the arrangement of an isopropyl group involves a large amount of essentially independent torsions. Because of this, there are far more conformers for $[(P(i\text{-}Pr)_3)_2Pd]$, and this results also in a wider range of conformational energies.

A random choice of conformers for each point along the reaction profile could give obviously quite bad results, so this is a good test case to evaluate the efficiency of more elaborate approaches still short of systematic conformational search. A first logical approach is the use of geometries similar to those from crystal structures. We decided to analyze the validity of this approach for **2is**. There are not many crystal structures available for L–M–$P(i\text{-}Pr_3)_2$ or *cis*- L_2–M–$P(i\text{-}Pr_3)_2$, and there is only one with a palladium metal centre: $(CO)_6Fe_3S_2Pd(P(i\text{-}Pr)_3)_2$ [64]. We took the isopropyl conformation of this X-ray structure and applied it to adduct **2is**. The species optimized starting from this conformation was located 1.1 kcal/mol above the lowest energy conformer of **2is.** The geometry is overall similar, yet not identical (the structure derived from X-ray presents a C_1–P_1–P_2–C_2 angle of 28.0° and Pd–P_i–C_i–H_i dihedral angles of −50.7 and 47.8°; to be compared with values for the most stable structure of 36.3°, −66.6 and 42.3°, respectively). The discrepancy between the two structures is likely associated with the different additional ligands involved. The advantages of using X-ray structures as starting point are nevertheless obvious. The use of this approach will however be limited by the availability of chemically similar X-ray structures, which can be especially difficult for sterically constrained transition states.

A second logical approach to reduce the problems associated with conformational diversity is to keep the system in the same conformation along the whole catalytic cycle. Although this may be difficult to implement when steric and electronic demands change along the reaction profile (i.e. linear $Pd(PR_3)_2$ vs. trigonal-planar adducts or *cis* vs. *trans* square-planar species), we evaluated the performance of this approach for the particular case of the energy difference between **2is** and **TSOAis**. The adducts corresponding to the six transition states **TSOAis a-f** were located at the QM level. The resulting barriers are 16.9, 16.9, 18.3, 17.7, 17.1 and 20.2 kcal/mol, respectively. These values are to be compared to the barrier between the lowest conformers of **TSOAis** and **2is**, which is18.2 kcal/mol. When attention is given to the connection between the species, the barriers still spread over a range of 3.3 kcal/mol (between 16.9 and 20.2 kcal/mol). This is a significant improvement from the 17.8 kcal/mol range obtained from randomly chosen conformers, but it is still a far from negligible error for a relatively elaborate procedure.

4 Conclusions

The results obtained in this study show the importance of conformational searches in the computational study of catalytic cycles. QM/MM calculations on the catalytic cycle of the Suzuki–Miyaura cross-coupling show that the error bars associated with conformational diversity range between 0.3 and 6.7 for the not so flexible $[(PPh_3)_2Pd]$ as catalyst, and between 10.2 and 11.4 kcal/mol for the more flexible $[(P(i\text{-}Pr)_3)_2Pd]$. These results have been confirmed by full QM calculations. Errors coming from choosing conformers at random could be for some systems quite large, of the same order or larger than the ones typically associated with a poor choice of DFT functional, or to the use of a too small basis set. These errors can be reduced by a careful choice of starting geometries, or by ensuring the different computed structures, but they cannot be fully suppressed without a systematic conformational search. An interesting consequence is that if the role of conformational diversity is neglected, the use of a larger model as PPh_3 can produce less accurate results than the use of a smaller, yet conformationally simpler, PMe_3. Conformational searches do not have to be mandatory, but their eventual need should be considered on a case by case basis.

Acknowledgments We thank the ICIQ foundation, the Spanish Ministerio de Ciencia e Innovacion (Consolider Ingenio 2010 CSD2006-0003 and CSD2007-000006; projects CTQ2008-06866-CO2-01/BQU, CTQ2008-06866-CO2-02/BQU, FEDER support), Generalitat de Catalunya (Grants 2009SGR0259 and XRQTC). M. B. thanks the Spanish Ministerio de Ciencia e Innovacion for a "Juan de la Cierva" grant.

References

1. Schwabe T, Grimme S (2008) Acc Chem Res 41:569
2. Bühl M, Reimann C, Pantazis DA, Bredow T, Neese F (2008) J Chem Theory Comput 4:1449
3. Sousa SF, Fernandes PA, Ramos MJ (2007) J Phys Chem A 111:10439
4. Rappe AK, Colwell KS, Casewit CJ (1993) Inorg Chem 32:3438
5. Comba P, Remenyi R (2003) Coord Chem Rev 238:9
6. Norrby PO, Brandt P (2001) Coord Chem Rev 212:79
7. Deeth RJ (2008) Inorg Chem 47:6711
8. Sabolovic J, Gomzi V (2009) J Chem Theory Comp 5:1940
9. Tubert-Brohman I, Schmid M, Meuwly M (2009) J Chem Theory Comp 5:530
10. Feldgus S, Landis CR (2000) J Am Chem Soc 122:12714
11. Landis CR, Feldgus S (2000) Angew Chem Int Ed 39:2863
12. Feldgus S, Landis CR (2001) Organometallics 20:2374
13. Ujaque G, Maseras F, Lledós A (1997) J Org Chem 62:7892
14. Ujaque G, Maseras F, Lledós A (1999) J Am Chem Soc 121:1317
15. Balcells D, Drudis-Sole G, Besora M, Dolker N, Ujaque G, Maseras F, Lledós A (2003) Faraday Discuss 124:429
16. Fey N (2010) Dalton Trans 39:296
17. Miyaura N, Yamada K, Suginome H, Suzuki A (1985) J Am Chem Soc 107:972
18. Miyaura N, Suzuki A (1995) Chem Rev 95:2457
19. Suzuki A (2002) J Organomet Chem 653:83
20. Christmann U, Vilar R (2005) Angew Chem Int Ed 44:366
21. Braga AAC, Ujaque G, Maseras F (2008) In: Musaev DG, Morokuma K (Org) Computational modeling for homogeneous and enzymatic catálysis: a knowledge-base for designing efficient catalysts. Wiley-VCH, Hoboken, NJ, pp 109–130
22. Molander GA, Canturk B (2009) Angew Chem Int Ed 48:9240
23. Xue L, Lin Z (2010) Chem Soc Rev 39:1692
24. Littke AF, Fu GC (2002) Angew Chem Int Ed 41:4176
25. Barrios-Landeros L, Hartwig JF (2005) J Am Chem Soc 127:6944
26. Kozuch S, Amatore C, Jutand A, Shaik S (2005) Organometallics 24:2319
27. Ahlquist M, Norrby PO (2007) Organometallics 26:550
28. Gourlaouen C, Ujaque G, Lledós A, Medio-Simón M, Asensio G, Maseras F (2009) J Org Chem 74:4049
29. Miyaura N (2002) J Organomet Chem 653:54
30. Gooßen LJ, Koley D, Hermann HL, Thiel W (2005) J Am Chem Soc 127:11102
31. Sicre C, Braga AAC, Maseras F, Cid MM (2008) Tetrahedron 64:7437
32. Ananikov VP, Musaev DG, Morokuma K (2005) Organometallics 24:715
33. Hartwig JF (2007) Inorg Chem 46:1936
34. Ananikov VP, Musaev DG, Morokuma K (2007) Eur J Inorg Chem 2007:5390
35. Pérez-Rodríguez M, Braga AAC, Garcia-Melchor M, Pérez-Temprano MH, Casares JA, Ujaque G, de Lera AR, Álvarez R, Maseras F, Espinet P (2009) J Am Chem Soc 131:3650
36. Hartwig JF, Paul F (1995) J Am Chem Soc 117:5373
37. Schoenebeck F, Houk KN (2010) J Am Chem Soc 132:2496
38. Ariafard A, Yates BF (2009) J Organomet Chem 694:1075
39. Ariafard A, Yates BF (2009) J Am Chem Soc 131:13981
40. Braga AAC, Ujaque G, Maseras F (2006) Organometallics 25:3647
41. Braga AAC, Morgon NH, Ujaque G, Maseras F (2005) J Am Chem Soc 127:9298
42. Braga AAC, Morgon NH, Ujaque G, Lledós A, Maseras F (2006) J Organomet Chem 691:4459
43. Mohamadi F, Richards NGJ, Guida WC, Liskamp R, Lipton M, Caufield C, Chang G, Hendrickson T, Still WC (1990) J Comp Chem 11:440
44. Chang G, Guida WC, Still WC (1989) J Am Chem Soc 111:4379
45. Saunders M, Houk KN, Wu YD, Still WC, Lipton M, Chang G, Guida WC (1990) J Am Chem Soc 112:1419
46. Allinger NL, Yuh YH, Lii JH (1989) J Am Chem Soc 111:8551
47. Shenkin PS, McDonald DQ (1994) J Comp Chem 15:899
48. Maseras F, Morokuma K (1995) J Comp Chem 16:1170
49. Vreven T, Morokuma K (2000) J Comp Chem 21:1419
50. Frisch MJ, Trucks GW, Schlegel HB, Scuseria GE, Robb MA, Cheeseman JR, Montgomery JJA, Vreven T, Kudin KN, Burant JC, Millam JM, Iyengar SS, Tomasi J, Barone V, Mennucci B, Cossi M, Scalmani G, Rega N, Petersson GA, Nakatsuji H, Hada M, Ehara M, Toyota K, Fukuda R, Hasegawa J, Ishida M, Nakajima T, Honda Y, Kitao O, Nakai H, Klene M, Li X, Knox JE, Hratchian HP, Cross JB, Bakken V, Adamo C, Jaramillo J, Gomperts R, Stratmann RE, Yazyev O, Austin AJ, Cammi R, Pomelli C, Ochterski JW, Ayala PY, Morokuma K, Voth GA, Salvador P, Dannenberg JJ, Zakrzewski VG, Dapprich S, Daniels AD, Strain MC, Farkas O, Malick DK, Rabuck AD, Raghavachari K, Foresman JB, Ortiz JV, Cui Q, Baboul AG, Clifford S, Cioslowski J, Stefanov BB, Liu G, Liashenko A, Piskorz P, Komaromi I, Martin RL, Fox DJ, Keith T, Al-Laham MA, Peng CY, Nanayakkara A, Challacombe M, Gill PMW, Johnson B, Chen W, Wong MW, Gonzalez C, Pople JA (2004) Revision C.02 ed. Gaussian, Inc., Wallingford, CT

51. Lee CT, Yang WT, Parr RG (1988) Phys Rev B 37:785
52. Becke AD (1993) J Chem Phys 98:5648
53. Stephens PJ, Devlin FJ, Chabalowski CF, Frisch MJ (1994) J Phys Chem 98:11623
54. Hehre WJ, Ditchfield R, Pople JA (1972) J Chem Phys 56:2257
55. Hariharan PC, Pople JÁ (1973) Theor Chim Acta 28:213
56. Francl MM, Pietro WJ, Hehre WJ, Binkley JS, Gordon MS, Defrees DJ, Pople JA (1982) J Chem Phys 77:3654
57. Dunning TH Jr, Hay PJ (1977) In: Schaefer III, HF (ed) Methods of electronic structure theory, vol 3. Plenum, New York, pp 1–28
58. Igelmann G, Stoll H, Preuss H (1988) Mol Phys 65:1321
59. Andrae D, Haussermann U, Dolg M, Stoll H, Preuss H (1990) Theor Chim Acta 77:123
60. Bergner A, Dolg M, Kuchle W, Stoll H, Preuss H (1993) Mol Phys 80:1431
61. Rappe AK, Casewit CJ, Colwell KS, Goddard WA, Skiff WM (1992) J Am Chem Soc 114:10024
62. Casado AL, Espinet P (1998) Organometallics 17:954
63. Tolman CA (1977) Chem Rev 77:313
64. Eremenko IL, Nefedov SE, Veghini DA, Rosenberger ST, Berke H, Ol'shnitskaya IA, Novotortsev VM (1997) Russ Chem Bull 46:137